ECEN 410 - Adv. Communications Engineering Project 2: Spatial Channel Models

David Dobbie

***Abstract*—This report compares two competing methodologies in modelling small scale fast fading for a single user MIMO (multiple input, multiple output) use case in wireless communications. Kronecker correlated fading and the Saleh-Valenzuela cluster models are compared for a 4×4 MIMO system representative of small-scale residential no line of sight (NLOS) wireless communications. We find that both models behave adversely differently from one another, making the Kronecker model appear to be not representative of MIMO systems.**

I. Introduction

MIMO in wireless communications opens up plenty of opportunity for spatial multiplexing made from the diversity potentially offered in a rich scattering environment [1]. Scattering in terms of wireless communications describes the multiple paths reflections of a signal take. This small scale variation is known as fading. The benefit in knowing this scattering principle is that we may understand how channel capacity is impacted by the physical environment.

II. Channel Models

We wish to compare the effects of spatial fading for small scale models so we will discount the adverse effects of path loss and shadowing by holding the mean received power constant. This model will deal with only single user MIMO for each resource user block. Multi-cell interference will also be assumed to be negligible. We will assume in addition that we will have a narrow-band flat fading system MIMO system to prevent time coherence from being an issue in analysis. Finally, we assume no channel state information at the transmitter (CSIT).

The following two channel models will describe the test two-dimensional system with no line of sight: the Classical Kronecker Correlated Fading Model, and the Saleh-Valenzuela Ray-Based Model.

A. Classical Kronecker Correlated Fading Model

The classical model has it's main benefits founded in the simplicity and mathematical tractability that it offers [2]. It may be expressed as:

$$\mathbf{H} = \sqrt{P}\mathbf{R}_r^{1/2}\mathbf{H}_{\text{iid}}, \mathbf{R}_t^{1/2}, \tag{1}$$

where $\mathbf{R}_r$ and $\mathbf{R}_t$ express the antenna correlations of the receiver and transmitter respectively and $\mathbf{H}_{\text{iid}}$ is a matrix of identical and independent Rayleigh – $\mathcal{CN}(0,1)$ – distributed values. This model reportedly holds for where:

- Tx with respect to Rx correlation coefficients are independent (and vice-versa), and
- cross correlations must equal the Tx and Rx [2] correlations.

For the correlation matrix's values, we will utilise a model proposed by Clerckx [3] such that:

$$\mathbf{R} = \begin{bmatrix} 1 & \rho & \rho^2 & \rho^3 \\ \rho & 1 & \rho & \rho^2 \\ \rho^2 & \rho & 1 & \rho \\ \rho^3 & \rho^2 & \rho & 1 \end{bmatrix} \tag{2}$$

where ρ the correlation constant between one antenna and another (for a 4×4 system). To further model phase change as well, the correlation constant itself is a random variable expressed as:

$$\rho = |\rho| e^{j\phi_i}, \tag{3}$$

where

$$\phi_i \sim U[0, 2\pi) \tag{4}$$

B. Saleh-Valenzuela Ray-Based Model

The ray-based model that this report will detail is one proposed by Saleh-Valenzuela. This will model a NLOS (not in the line of sight) channel [4].

The overall channel impulse response for the ray based model is defined as:

$$\mathbf{H} = \sqrt{P}\sum_{c=1}^{C}\sqrt{\frac{\gamma_c}{L}}\sum_{l=1}^{L} h_{\text{iid},c,l}\mathbf{a}_{\text{RX}}(\varphi_{c,l}^{\text{AOA}})\mathbf{a}_{\text{TX}}(\varphi_{c,l}^{\text{AOD}}) \tag{5}$$

where the receiving response antenna vector, $\mathbf{a}_{\text{RX}}(\varphi_{c,l}^{\text{AOA}})$, is:

$$\mathbf{a}_{\text{RX}}(\varphi_{c,l}^{\text{AOA}}) = \begin{bmatrix} 1 \\ e^{j2\pi\Delta cos(\varphi^{\text{AOA}})} \\ e^{j2\pi(2)\Delta cos(\varphi^{\text{AOA}})} \\ \vdots \\ e^{j2\pi(N_r-1)\Delta cos(\varphi^{\text{AOA}})} \end{bmatrix} \tag{6}$$

and the transmitting response antenna vector, $\mathbf{a}_{\text{TX}}(\varphi_{c,l}^{\text{AOD}})$, is:

$$\mathbf{a}_{\text{TX}}(\varphi_{c,l}^{\text{AOD}}) = \begin{bmatrix} 1 \\ e^{j2\pi\Delta cos(\varphi^{\text{AOD}})} \\ e^{j2\pi(2)\Delta cos(\varphi^{\text{AOD}})} \\ \vdots \\ e^{j2\pi(N_t-1)\Delta cos(\varphi^{\text{AOD}})} \end{bmatrix} \tag{7}$$

1) Variables: The variables that make up the model in (5) are:

- $\mathbf{H}$ is the impulse response between each of the receiving and transmitting antennas,
- P is the power of the overall channel,
- $c \in \{1, \dots C\}$ are the indices of each of the clusters,
- $l \in \{1, \dots L\}$ are the indices of each of rays associated with each cluster,
- γ_c is the power of each cluster,
- $h_{\text{iid},c,l} \sim \mathcal{CN}(0,1)$ is a Rayleigh distribution for each of the rays,
- $\mathbf{a}_{\text{TX}}(\varphi_{c,l}^{\text{AOD}})$ describes the angle of departure (AOD) from each antenna on the transmitter to the departing rays,
- $\mathbf{a}_{\text{RX}}(\varphi_{c,l}^{\text{AOA}})$ describes the angle of arrival (AOA) from each antenna on the receiver to the arriving rays,
- ϕ_c is the central cluster angle,
- Δ is the separation between each of the antenna (equal spacing is assumed).

To attain an accurate portrayal of typical performance, several components of the model will be stochastic. They are that:

- φ_{cl} is the summation of two instantiations of random variables such that $\varphi_{cl} = \phi_c + \Delta_{cl}$
- $\Delta_{cl} \sim \mathcal{L}(\sigma_s^2)$ is the Laplace distributed offset angle of each ray from the central cluster angle.

The power of each cluster is described by:

$$\gamma_c^{'} = \sqrt{\beta_c} e^{j\Phi_c} \tag{8}$$

where,

$$\Phi_c \sim \mathcal{U}[0, 2\pi) \tag{9}$$

is the cluster's phase coefficient (where ϕ_c is an instantiation of this variable), and

$$\beta_c = L d^{-n}. \tag{10}$$

describes the power for each cluster.

In (10), d^{-n} corresponds to cluster path loss from the receiver due to separation distance. The L term is the log-normal shadow fading of the cluster power, i.e. $log(L) \sim \mathcal{N}(0, \sigma_{\text{cluster}})$. Furthermore, we will let $d \sim \mathcal{U}[0, d_{\text{max}}]$ so that we may model clusters of varying distance away from the user. The combination of random cluster distances and angles means we can average over a series of different cluster positions relative to the user, ensuring generality.

To make the models comparable, all of the cluster powers are normalised such that their average power is unity. As in:

$$\gamma_c = \frac{\gamma_c^{'}}{\sum_{c=1}^{C} \gamma_c^{'}} \tag{11}$$

2) Constants: The channel model characteristics will adopt some of the low power wireless model proposed for IEEE 802.15.4a for a residential environment [5] with angles derived from the 3GPP standard for an indoor hot-spot (InH) [6]. The constants are detailed in Table I. The antenna distance corresponds to half the wavelength of 2.4GHz communications used for IEEE 802.11.ac [7].

Constant	Value	
n	Cluster Path Loss	4.58
σ_{cluster}	Cluster Shadowing	3
σ_s	Offset Angle Std. Dev.	5°
Δ	Antenna Distance	62.5 mm
C	Cluster count	19
L	Ray count	20

TABLE I: Constants for the wireless channel model

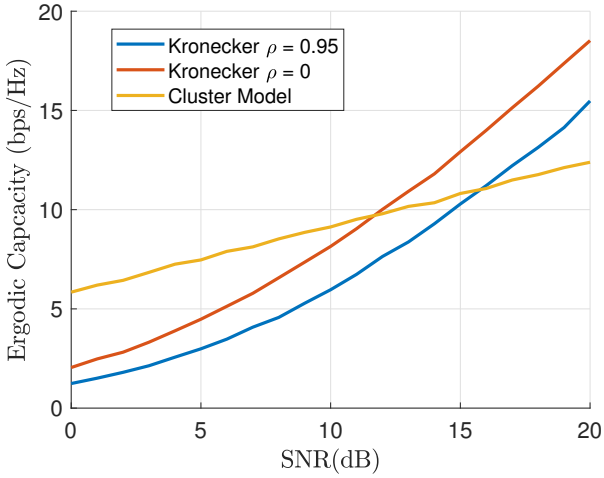

Fig. 1: Ergodic capacity of the channel models for varying SNR

III. Results and Analysis

We will examine the different channel models in terms of how their channel capacities compare. We will examine outage capacity at a channel power and ergodic capacity for different SNR. As there is no CSIT, the channel capacity expression is:

$$C = \log|\mathbf{I} + \frac{1}{n_T}\mathbf{H}\mathbf{H}^H| \tag{12}$$

The channel power term, P, is embedded in the channel term $\mathbf{H}$. This will be the variable that will be changed to obtain the capacity with respect to received SNR.

A. Simulation

The analysis will be a Monte Carlo analysis of 1×10^3 instances of the channel $\mathbf{H}$. This appears to be sufficient to achieve convergence for the comparable plots.

B. Ergodic Capacity

In Figure 1 we observe that the cluster model behaves significantly differently to the Kronecker model for both correlations tested. This implies that the Kronecker model underestimates the ergodic capacity by over half at $SNR = 0$ and overestimates for higher SNRs. This implies adverse effects for modelling cell edge reliability constraints.

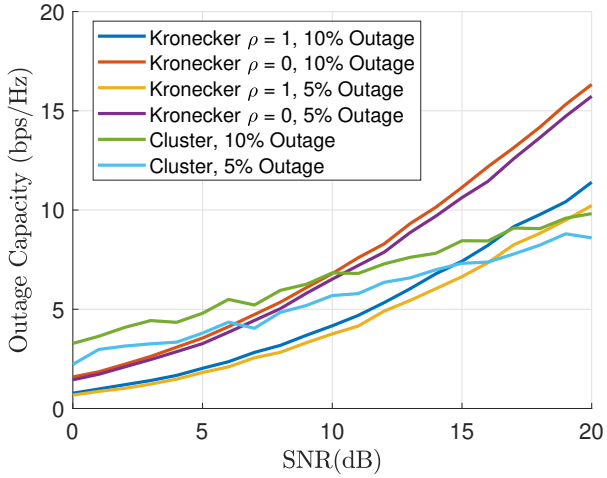

Fig. 2: Outage capacity of the channel models for varying SNR

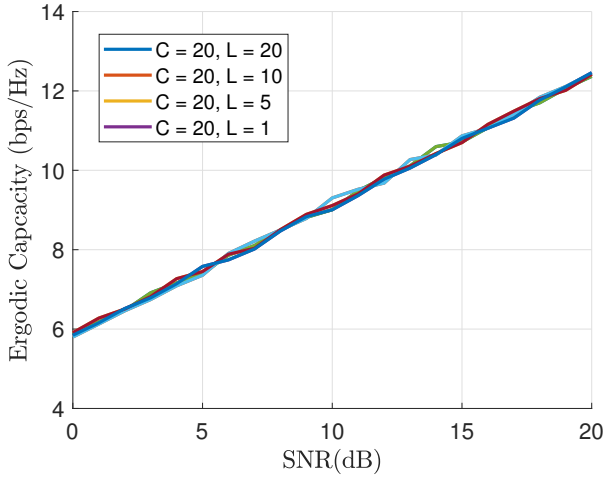

Fig. 3: Ergodic capacity for different counts of rays

C. Outage Capacity

With the outage capacity we gain a perspective for dealing with cell edge reliability. Figure 2 reveals that the highly correlated Kronecker capacity underestimates the cluster outage for an SNR below 16dB. The linear trend of the outage capacity of the cluster models furthermore imply that the power of the signal and correlation between antennas are not linked as tightly, unlike the Kronecker model.

D. Sensitivity to Cluster, Ray Count

We are motivated to see how capacity changes with respect to the number of clusters and ray per cluster given. In Figure 3 we observe no significant deviation of the capacity for different ray counts. This indicates that the performance improvement of fast fading comes from high position diversity of the clusters rather than the smaller deviation of the rays.

The effect of the number of clusters is revealed by Figure 4 where we vary the clusters count. We see that once the cluster count drops below 5, we see a marked reduction in performance. This is corresponds to a reduced gain due to low

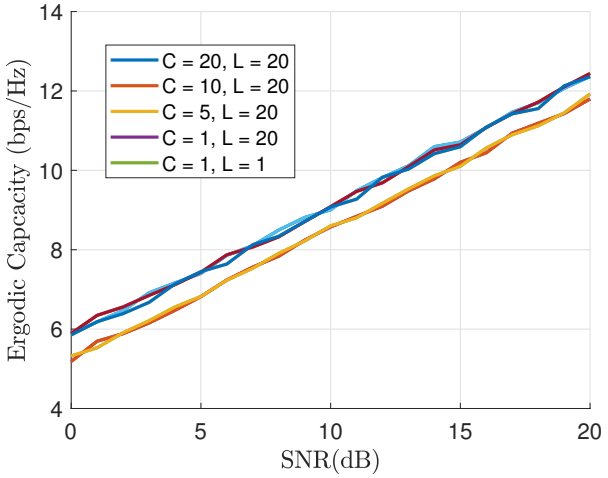

Fig. 4: Ergodic capacity for different counts of clusters

spatial diversity. The multiple antennas are more correlated as they have little difference in their received signal.

IV. Conclusion

This comparative study has revealed that the classical Kronecker model performs poorly in estimating the channel capacity of a system for low received SNR. This means that designing for cell-edge reliability with a known environment requires the cluster model to obtain a more representative result.

References

[1] C.-X. Wang, X. Hong, H. Wu, and W. Xu, "Spatial-temporal correlation properties of the 3gpp spatial channel model and the kronecker mimo channel model," *EURASIP Journal on Wireless Communications and Networking*, vol. 2007, no. 1, p. 039871, 2007.

[2] C. Oestges, "Validity of the kronecker model for mimo correlated channels," in *Vehicular Technology Conference, 2006. VTC 2006-Spring. IEEE 63rd*, vol. 6. IEEE, 2006, pp. 2818–2822.

[3] B. Clerckx, G. Kim, and S. Kim, "Correlated fading in broadcast mimo channels: Curse or blessing?" in *Global Telecommunications Conference, 2008. IEEE GLOBECOM 2008. IEEE*. IEEE, 2008, pp. 1–5.

[4] A. A. Saleh and R. Valenzuela, "A statistical model for indoor multipath propagation," *IEEE Journal on selected areas in communications*, vol. 5, no. 2, pp. 128–137, 1987.

[5] A. F. Molisch, K. Balakrishnan, D. Cassioli, C.-C. Chong, S. Emami, A. Fort, J. Karedal, J. Kunisch, H. Schantz, U. Schuster *et al.*, "Ieee 802.15. 4a channel model-final report," *IEEE P802*, vol. 15, no. 04, p. 0662, 2004.

[6] "3GPP TR 36.873 v12.7.0 (2017-12)." 3rd Generation Partnership Project, 2017, p. 35. [Online]. Available: http://www.3gpp.org/ftp//Specs/archive/36_series/36.873/36873-c70.zip

[7] E. Perahia and M. X. Gong, "Gigabit wireless lans: an overview of ieee 802.11 ac and 802.11 ad," *ACM SIGMOBILE Mobile Computing and Communications Review*, vol. 15, no. 3, pp. 23–33, 2011.